Reaction dynamics in the ^{58}Ni+^{58}Ni system at intermediate energies.

Lucia Baldesi

The African Nuclear Physics Conference 2025
24-28 November 2025

INDRA FAZIA

UNIVERSITÀ DEGLI STUDI FIRENZE

INFN
Istituto Nazionale di Fisica Nucleare

NUCLEX

Physics case

Heavy-Ion collision in the Fermi energy domain

Semiperipheral collisions at **intermediate energies** ($20<E_{beam}<100$ AMeV):

- **The dominant channel is the binary one:** formation of two excited fragments, which preserve memory of the entrance channel.

  In the ejectiles we observe the superposition of two effects:
  - **Statistical**: decay from a thermodynamically equilibrated source
  - **Dynamical**:
    - emission towards midvelocity → neck
    - Neutron enrichment of the midvelocity

- Another possible exit channel is the **dynamical breakup** of the QP and/or QT.

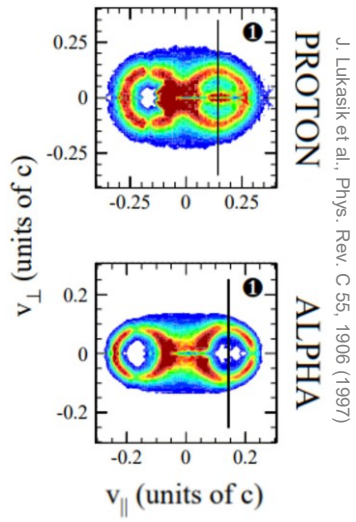

J. Lukasik et al., Phys. Rev. C 55, 1906 (1997)

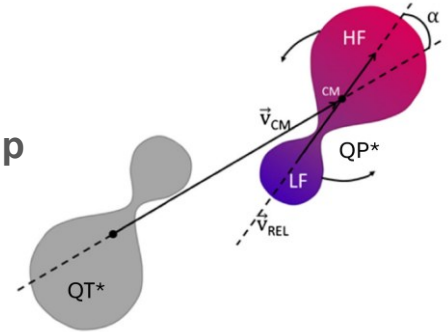

A. Jedele et al., Phys. Rev. Lett. 118, 062501 (2017)

BNV calculation of density contour plots

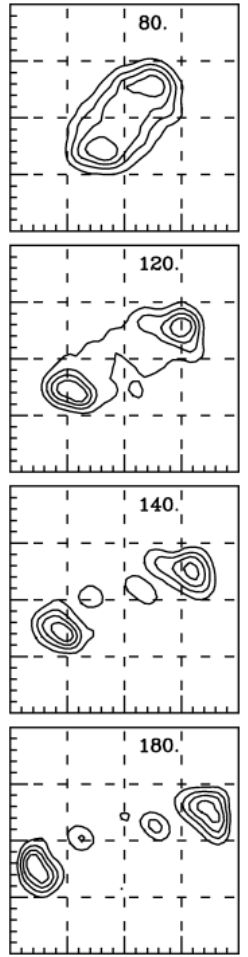

V. Baran et al., Nucl. Phys. A 703, 603 (2002).

Physics case

Heavy-Ion collision and the isospin drift

An experimental observation is the **neutron enrichment of the neck**, which can be interpreted in the framework of the **nuclear Equation of State**

$$\frac{E}{A}(\rho, I) = \frac{E}{A}(\rho) + \frac{E_{sym}}{A}(\rho) I^2$$

$$I = \frac{N - Z}{A}$$

$$\rho = \rho_n + \rho_z$$

→ Symmetric matter

→ Asymmetric matter

V. Baran et al. / Physics Reports 410 (2005) 335 – 466

$$\frac{E}{A}(\rho) = E_{sat} + \frac{1}{2} K_{sat} x^2 + \ldots \qquad x = \frac{\rho - \rho_0}{\rho_0}$$

$$\frac{E_{sym}}{A}(\rho) = E_{sym} + L_{sym} x + \frac{1}{2} K_{sym} x^2 + \ldots$$

The symmetry energy produces a difference of the proton and neutron currents:

$$j_n - j_p \propto \frac{E_{sym}}{A}(\rho) \nabla I + \frac{\partial E_{sym}/A}{\partial \rho} \nabla \rho$$

Isospin Diffusion:

- driven by the isospin gradient
- tends to equilibrate neutron–proton imbalance.

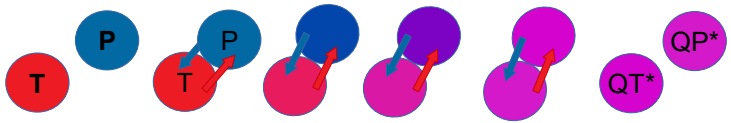

Isospin Drift:

- driven by the density gradient.
- induces a net neutron flux towards low density regions

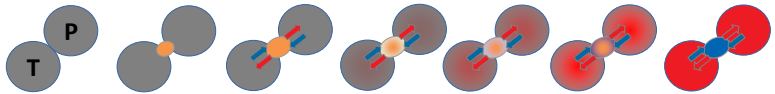

Physics case

^{58}Ni+^{58}Ni @ 32, 52 and 74 AMeV

^{58}Ni+ ^{58}Ni at 32, 52 and 74 AMeV: evolution of the dynamics with incident energy and centrality in semipheripheral collisions.

- QP pahse space: selection of the QP evaporative (**QPr**) and the QP breakup (**QPb**) channels

- Centrality estimator:

  reduced momentum $p_{red} = \left(\frac{p_z^{QP}}{p_{beam}}\right)$

- From the cold detected fragments, we aim at infer information on the dynamical phase:
  - **Primary source reconstruction**: size and excitation energy of the primary QP* and the neck source
  - **Isospin drift:** isospin investigation of the evaporative and midvelocity emissions

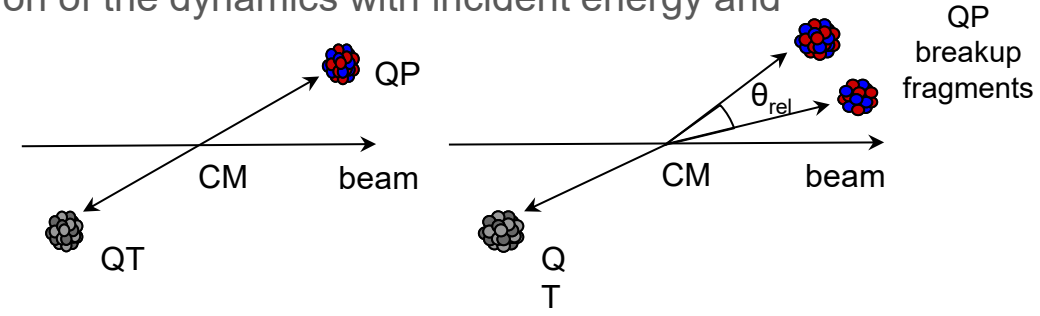

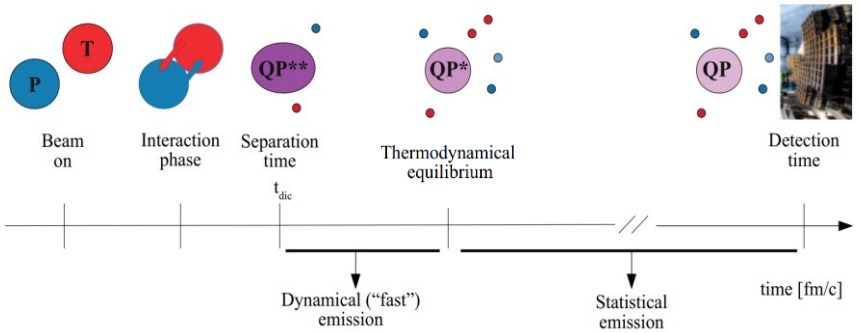

Experimental setup

The INDRA-FAZIA apparatus

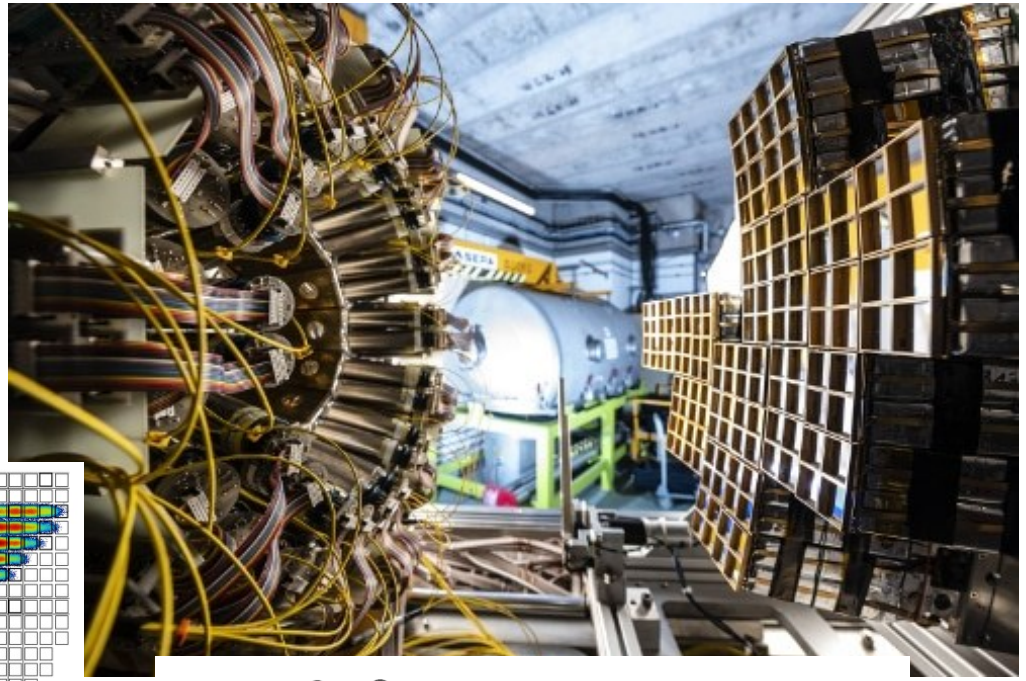

INDRA

- 12 rings covering from 14° to 176°
- Charge discrimination up to uranium, mass discrimination up to Z ~ 10.

FAZIA

- 12 blocks covering from 2° to 14°.
- Charge discrimination up to uranium, isotopic discrimination up to Z ~ 25

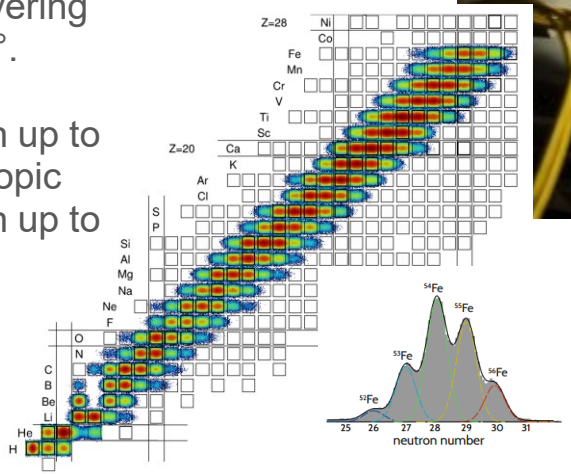

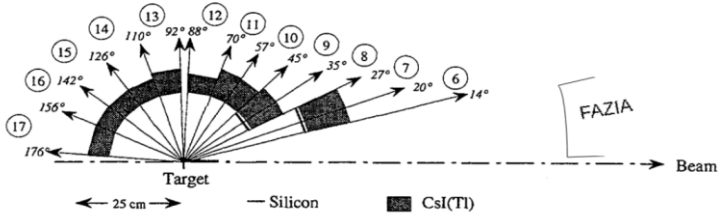

Secondary fragments

- **Quasi-projectile** (remnant or reconstructed)

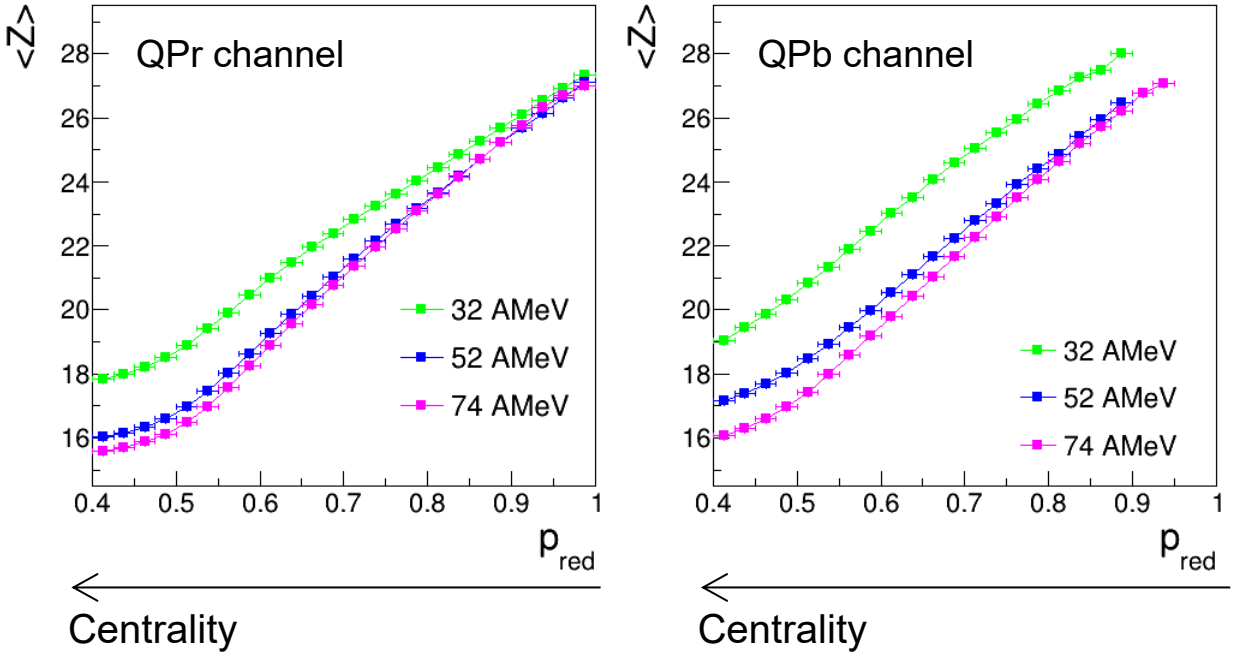

Secondary fragments

- Quasi-projectile (remnant or reconstructed)
- **Light charged fragments (Z<5)**
  - **QP phase space**: selection of fragments (identified in mass) emitted in the forward hemisphere of the centre of mass reference frame (not-dashed region)
  - **Efficiency correction**: obtained using AMD+GEMINI++ simulations

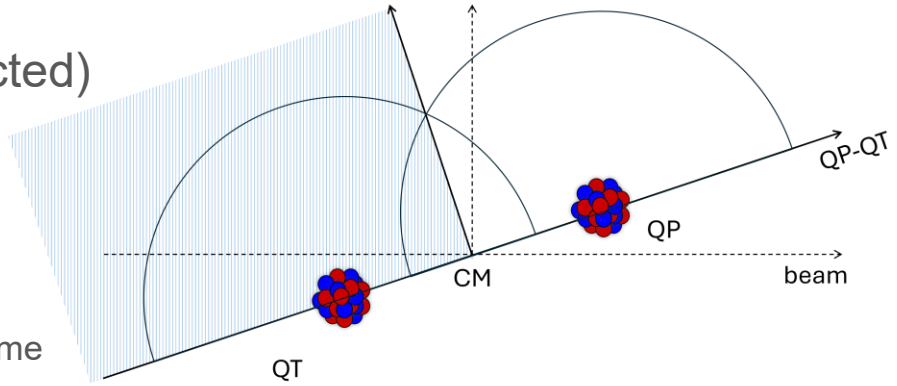

protons @ 74 AMeV (p_{red}=0.6-0.7)

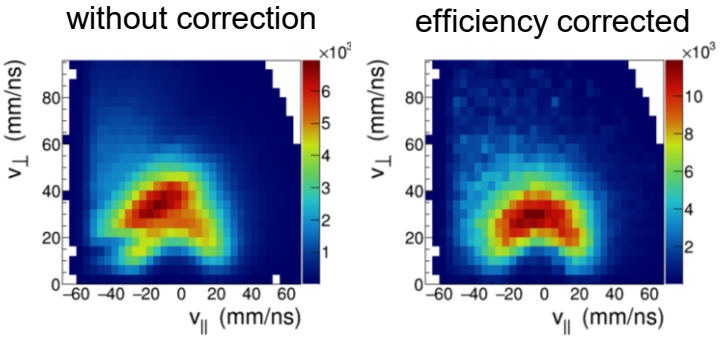

^{58}Ni+^{58}Ni @ 74 AMeV

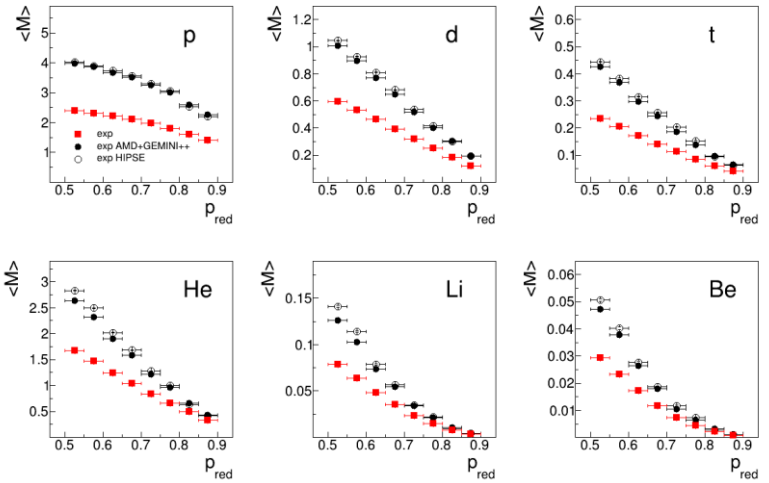

Secondary fragments

- Quasi-projectile (remnant or reconstructed)
- Light charged fragments (Z<5)
- **Free neutrons**
  - Not detected
  - The average number of free neutrons can be estimated as the difference between the Nproj and the <N> estimated considering the bounded neutrons.

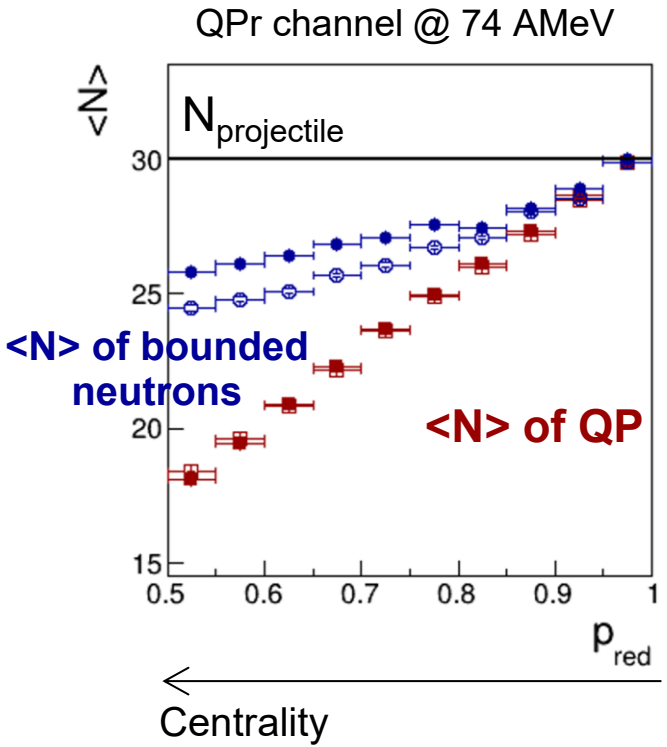

Disentanglement between evaporative and midvelocity emissions

- **Yields**

S. Piantelli, PRC 74, 034609 (2006)
A. Mangiarotti, PRL 93, 232701 (2004)

  - **Light charged fragments:**
    - angular distributions of θ, i.e. the polar angle between the charged particle in the QP frame and the QP-QT separation axis
      → superposition of two emission components
      - **statistical evaporation**: approximately a sin(θ) distribution
      - large excess at backward angles which is ascribed to **midvelocity emission**.
  - **Free neutrons:**
    - hypothesis must be done

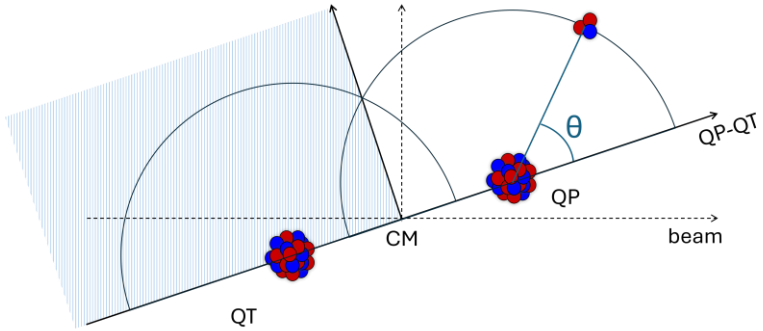

^{58}Ni+^{58}Ni @ 74 AMeV

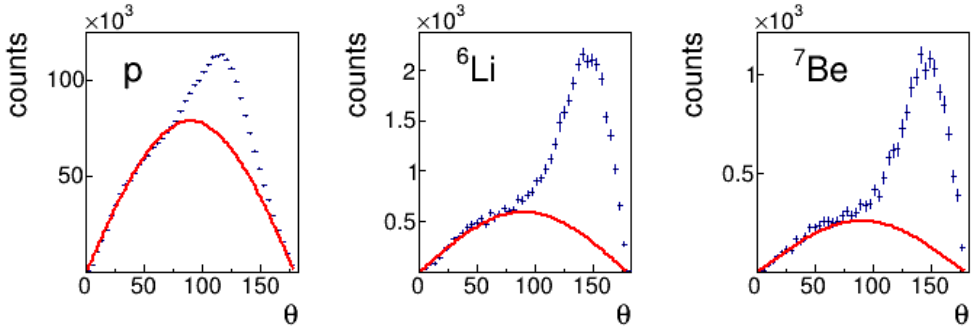

- **Energies:**
  - Nuclear calorimetry technique

Primary source characteristics

QP* source

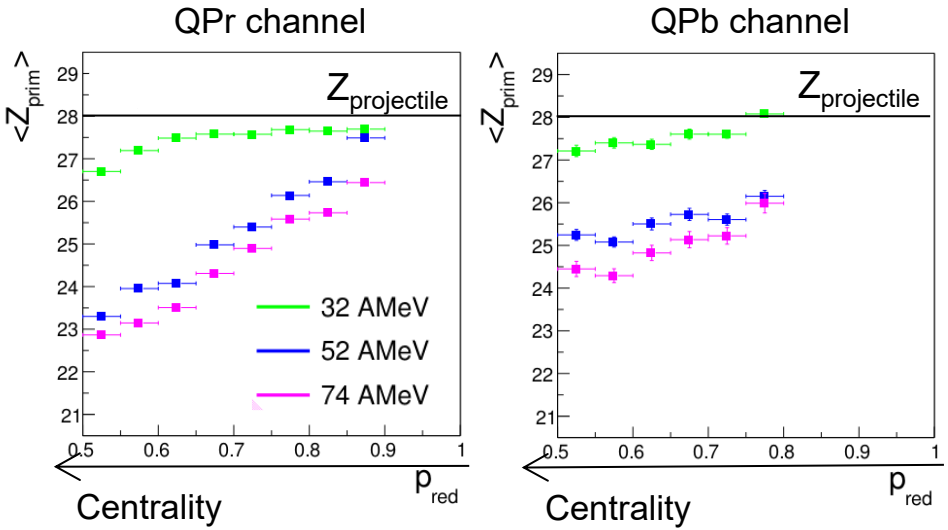

- the size of the QP* depends on both centrality and incident energy: the QP* remains close to the projectile at 32 AMeV, but becomes much lighter in central collisions at 52 and 74 AMeV

neck source

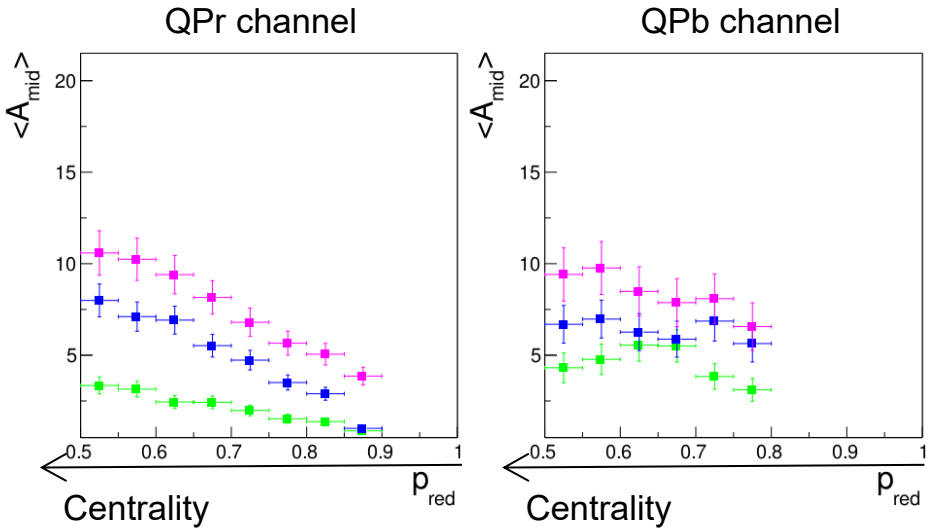

- the midvelocity contribution increases with centrality and clearly grows with beam energy

Primary source characteristics

QP* source

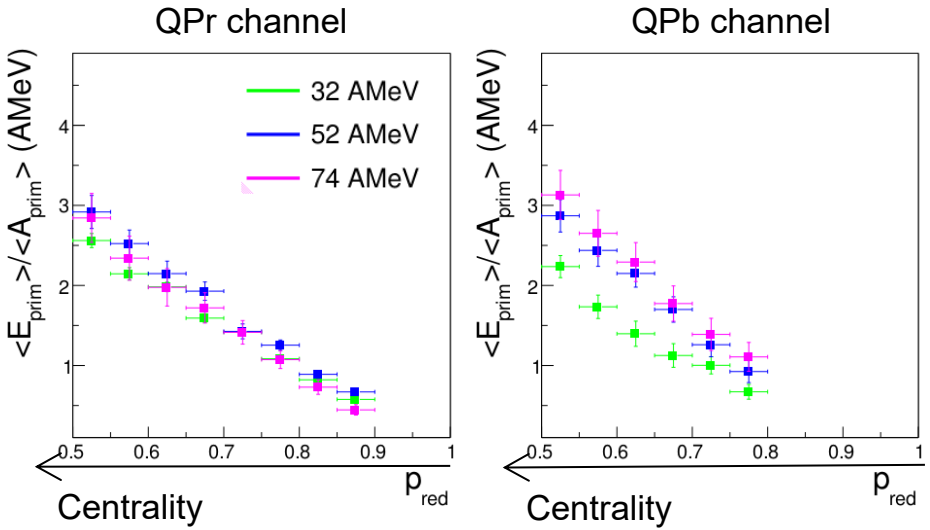

- the excitation energy per nucleon of the QP*, as expected for an equilibrated source, remains below 3 AMeV and increases with centrality

neck source

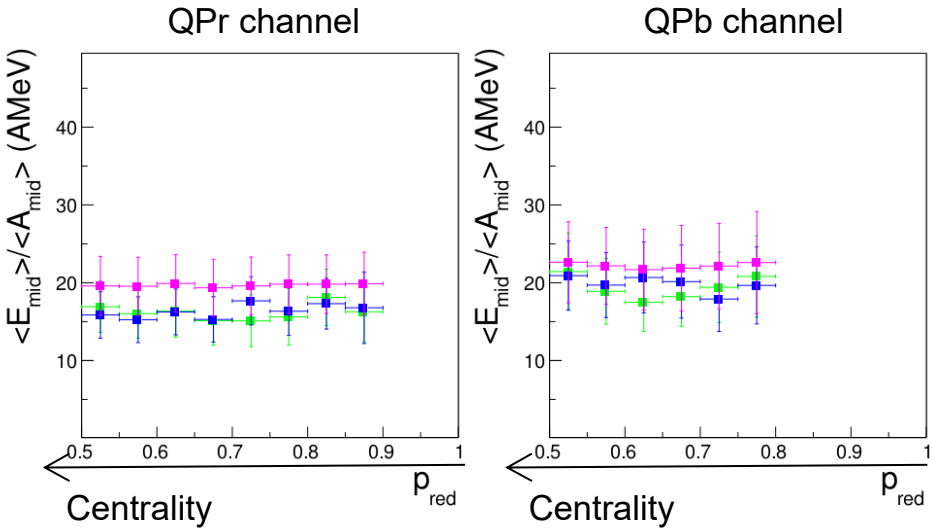

- the energy density of the neck source is significantly higher (~15-20 AMeV) and shows no dependence on either centrality or beam energy.

Primary source characteristics

Comparison with the AMD+GEMINI++ simulations

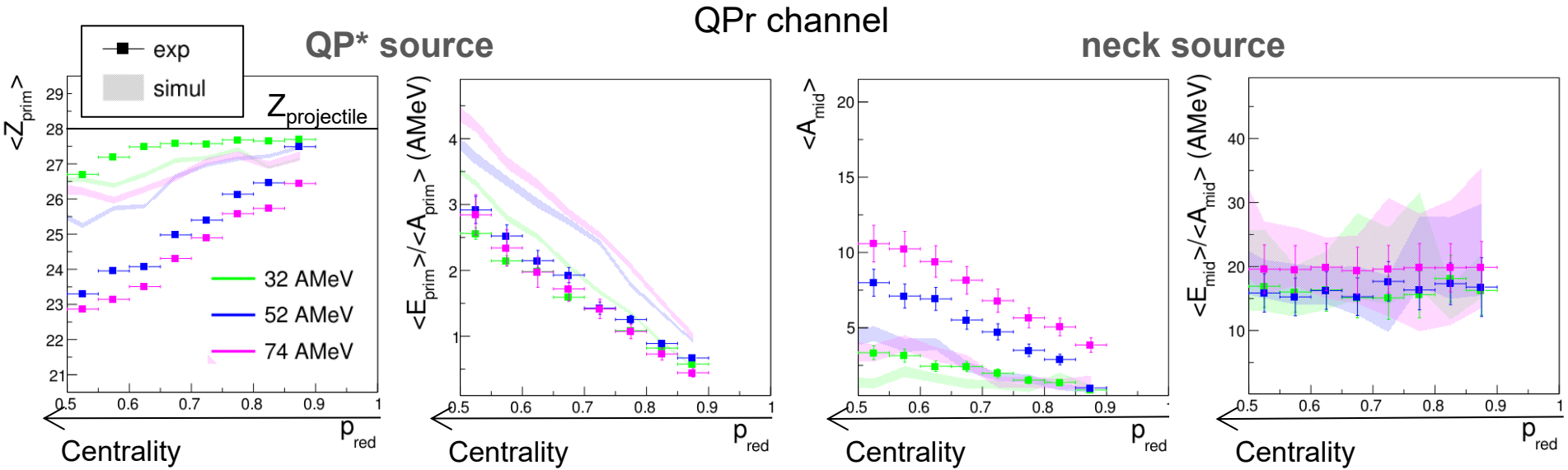

- overall satisfactory reproduction of the secondary fragment characteristics
- differences in the properties of the primary sources: underestimation of the midvelocity contribution
- Within AMD, the properties of the primary QP* source can be independently evaluated as a function of time → the proposed reconstruction procedure allows to approach the characteristics of the fragments at the end of the dynamical stage (150-300 fm/c).

Isospin drift

isospin ratio for complex particles: $\langle N\rangle/\langle Z\rangle_{CP} = \sum_i \sum_\nu N_\nu^i / \sum_i \sum_\nu Z_\nu^i,$

E. Galichet, PRC 79, 064614 (2009)

- where the v index numbers the different complex particles in the ith event, and the outer sum runs over all the events in the selected pred bin.
- d, t, ^{3}He, ^{4}He, ^{6}He, ^{6}Li, ^{7}Li, ^{8}Li, ^{9}Li, ^{7}Be, ^{9}Be, and ^{10}Be are taken into account as complex particles
- free protons and neutrons are excluded

QPr channel

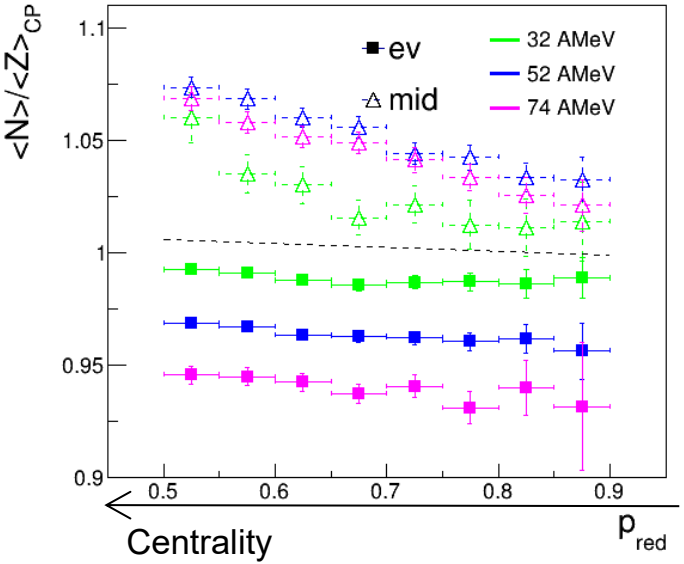

- the **neutron enrichment of the neck** is clearly observed
- midvelocity emission: the N/Z is essentially independent on the beam energy.
- evaporative component: an interesting dependence on the beam energy emerges.
  - different isospin content of the QP* source which reflects on the evaporated particles
  - as the energy increases, the growing midvelocity contribution leaves the QP* slightly more neutron poor
- Since the neutron enrichment of the midvelocity component weakly depends on the beam energy, this effect in mainly driven by the increasing abundance of midvelocity yields.

Conclusions

- Experimental access to the dynamical phase (150-300 fm/c) in both the QPr and QPb channels
- Similar results in the two channels → following evolution of the QP* largely independent of its size and excitation energy.
- Primary source reconstruction
  - The excitation energy of the primary QP* is below 3 AMeV
  - The midvelocity contribution increases with the incident energy
  - The energy density of the neck source is 15-20 AMeV → dynamical origin from a hot overlapping region
  - The AMD+GEMINI++ simulations underestimate the midvelocity contribution
- Isospin Drift
  - The neutron enrichment of the neck is clearly observed
  - The midvelocity emission plays a key role in determining the isospin characteristics of the primary QP*, mainly driven by the increasing amount of neck emissions.

Thank you for your attention

INDRA FAZIA

NUCLEX

INFN

Istituto Nazionale di Fisica Nucleare

UNIVERSITÀ DEGLI STUDI FIRENZE